Journal of the Mechanical Behavior of Biomedical Materials 95 (2019) 172–179

Contents lists available at ScienceDirect

Journal of the Mechanical Behavior of Biomedical Materials

journal homepage: www.elsevier.com/locate/jmbbm

Newer vs. older CAD/CAM burs: Influence of bur experience on the fatigue behavior of adhesively cemented simplified lithium-disilicate glass-ceramic restorations

Guilherme Schmitt de Andrade[a], Vandeberg Diniz[a], Carlos Eduardo Datte[a], Gabriel Kalil Rocha Pereira[c], Andressa Borin Venturini[b], Tiago Moreira Bastos Campos[e], Marina Amaral[d], Marco Antonio Bottino[a], Luiz Felipe Valandro[b,*], Renata Marques de Melo[a]

[a] Department of Dental Materials and Prosthodontics, São Paulo State University (Unesp) – Institute of Science and Technology, São José dos Campos, Brazil
[b] Oral Science, Prosthodontics Unit, Faculty of Odontology, Federal University of Santa Maria (UFSM), Santa Maria, Brazil
[c] School of Dentistry, Meridional Faculty-IMED, Passo Fundo, Rio Grande do Sul State, Brazil
[d] Department of Dentistry (Prosthetic Dentistry), University of Taubaté (UNITAU), Taubaté, Brazil
[e] Department of Physics, Aeronautical Technology Institute (ITA), São José Dos Campos, Brazil

ARTICLE INFO

Keywords:
Fatigue
Machining
Roughness
All-ceramic
Radial crack
Cementation

ABSTRACT

This study evaluated the effect of the CAD/CAM burs experience (newer vs older as consequence of the milling sequence) on fatigue failure load (FFL), number of cycles for failure (CFF), and survival rates of lithium disilicate glass-ceramic simplified restorations adhesively cemented to a dentin analogue substrate. Three sets of CAD/CAM burs were used to mill disc-shaped ceramic specimens (1 bur set – 18 milled discs with 10 mm diameter and 1.5 mm thickness), considering the bur experience as a result of the milling sequence to compose the study groups: G1-6 – discs obtained from the 1st to 6th milling of each bur set; G7-12 – specimens from the 7th to 12th milling; G13-18 – discs from the 13th to 18th. Discs of dentin analogue (G10, 10 mm diameter and 2.0 mm thickness) were made to serve as substrate (base material) and randomly assigned into pairs with the respective ceramic discs. Then, the ceramic discs were adhesively cemented onto the dentin analogue substrate, composing a three-layer specimen that mimics a monolithic restoration of a posterior tooth. Specimens were tested under stepwise fatigue approach: frequency = 20 Hz, 5000 cycles at maximum load of 400 N to accommodate the testing assembly, followed by incremental steps of 200 N with initial load ranging from 10 to 1000 N, to a maximum of 20,000 cycles/each step, until the occurrence of failure (radial crack). FFL and CFF were recorded at the end of the testing and subjected to statistical analysis. Supplementary roughness analysis of the milled surface was performed (n = 18) using a contact profilometer. Residual stress after milling and acid etching were accessed via X-ray Diffractometry analysis. FFL and CFF were not affected by increase on bur experience (no statistical differences among groups), despite that, it affected both Ra and Rz parameters (G1-6 had the smoothest surface). The residual stress concentration was negligible (milling did not induce residual stress concentration). It is concluded that the fatigue behavior of adhesively cemented lithium-disilicate glass-ceramic restorations was not influenced by CAD/CAM bur experience (newer vs older as consequence of the milling sequence), and so the residual stress concentration induced by milling was negligible.

1. Introduction

The technological advances in CAD/CAM systems have stimulated manufacturers and researchers to develop new materials with high aesthetic performance and better biomechanical properties (Li et al., 2014). An advantage of the CAD/CAM technology is that the ceramic

* Corresponding author. Federal University of Santa Maria Faculty of Odontology, Oral Science, Prosthodontics Units, Floriano Peixoto, 1184, 97015-372, Santa Maria, RS, Brazil.
E-mail addresses: guilherme.andrade@ict.unesp.br (G. Schmitt de Andrade), vandebergdiniz@gmail.com (V. Diniz), cedatte@gmail.com (C.E. Datte), gabrielkrpereira@hotmail.com (G.K.R. Pereira), andressa.venturini@hotmail.com (A.B. Venturini), moreiratiago22@gmail.com (T.M.B. Campos), marinamaral_85@yahoo.com.br (M. Amaral), mmbottino@uol.com.br (M.A. Bottino), valandrolf@gmail.com (L.F. Valandro), marquesdemelo@gmail.com (R. Marques de Melo).

https://doi.org/10.1016/j.jmbbm.2019.04.002
Received 20 February 2019; Received in revised form 2 April 2019; Accepted 5 April 2019
Available online 09 April 2019

blocks are processed under industrial conditions, resulting in a more homogeneous material with fewer defects and cracks incorporated in its structure (Beuer et al., 2008; Denry and Kelly, 2014; Jokstad, 2017). However, literature supports that the milling process may also include defects or flaws on the ceramic surface and sub-surfaces, altering the integrity of the fabricated blocks (Alao et al., 2017; Lebon et al., 2015; Zhang et al., 2006).

These defects/flaws in micron/submicron scales originate from the abrasive diamonds of the milling cutters. The more abrasive the cutting instruments, the larger the population and the depth of the defects (Curran et al., 2017). This is critical, in particular for glass-ceramics due to their brittle nature, as increases in flaws leads to a decrease in resistance to crack propagation (Teixeira et al., 2007). Also, the higher the hardness of the ceramic, the greater the surface roughness and the deterioration of the milling cutter (Lebon et al., 2015). Along with milling of ceramic pieces using the same pair of diamond burs, the cutting capacity (removal of ceramic material from the blocks) of the burs might change, which influences the surface features and mechanical behavior of the ceramic, even though a recent study (Madruga et al., 2019) showed that sequential CAD/CAM bur usage had no effect on the fatigue strength of lithium disilicate glass-ceramic when testing monolithic samples under biaxial flexure fatigue test (cyclic loading).

Corazza et al. (2015) evaluated the effect of bur deterioration used in the milling process on the surface morphology and its consequences on the fatigue strength of a zirconia-based ceramic material adhesively cemented to dentin analogue, and only observed an influence of milling order on the surface roughness. However, zirconia ceramics present a polycrystalline microstructure, being less prone to slow-crack growth than glass-ceramics such as lithium disilicate (Wendler et al., 2018). Also, milling Y-TZP materials is considered 'soft-milling' since they are milled in a pre-sintered stage. Therefore, it is different from lithium disilicate glass-ceramic block milling, which is known as 'hard-milling' because these blocks are already sintered when milling occurs, while they are only subjected to the final crystallization process after milling (Fraga et al., 2015). Thus, the 'hard-milling' process is more susceptible to defects and cracks.

Another important factor in the mechanical performance of ceramic restorations is the strengthening effect promoted by resin adhesive cementation of ceramic materials (Anami et al., 2016; Campos et al., 2017; Kelly et al., 1996; Monteiro et al., 2018). The hydrofluoric acid etching of glass-ceramic surfaces and resin cement bonding can minimize the influence of flaws on cementation surfaces since acid etching may round or smooth the defects, while the resin cement penetrates into irregularities, sealing small failures ('healing' effect) (Prochnow et al., 2018a,b; Venturini et al., 2017). The sealing promoted by silane and resin cement also inhibits water uptake and ceramic degradation (Anusavice and Hojjatie, 1992; Kelly et al., 1996).

Although ceramics fracture under intense and sudden loads such as the loads applied in monotonic tests, clinical failures occur under cyclic loading (mechanical fatigue effect) different from the higher loads reported in *in vitro* studies. The intra oral cyclic loading associated to a humid environment lead to stress concentration around defects, which make crack propagation from the flaws more probable until threshold fracture of the structure (Kelly, 1999; Zhang et al., 2013). Ceramics can resist well against compressive loads, but occlusal compression loads lead to ceramic bending and tensile stress concentration on the cementation surface, inducing radial cracks from this region (either at defects/flaws in the resin cement (bubbles, for instance) or ceramic surface) (Anusavice and Hojjatie, 1992; Kelly, 1999; Kelly et al., 1990; Thompson et al., 1994; Zhang et al., 2013; Anami et al., 2016; Campos et al., 2017; Kelly et al., 1996; Monteiro et al., 2018; Prochnow et al., 2018a,b; Venturini et al., 2017). Sample failure must be similar to those found clinically in order to make *in vitro* results more clinically relevant (Gressler May et al., 2015; Kelly, 1999). From this standpoint, the fatigue tests represent the best method to mimic the clinical scenario, since cyclical intermittent loading under low loads leads to mechanical fatigue phenomenon, i.e. low tensile stress leading to a forward slow crack growth (Suresh, 1991).

Considering the aforementioned premises, one question still remains: might the increased bur experience as a result of milling sequence (newer Vs older burs) of lithium disilicate glass-ceramic restorations affect the mechanical fatigue behavior (under cyclic loading) of the restorations when cemented on the dentin analogue substrate? Thus, the aim of this study is to evaluate if the sequential use of CAD/CAM burs (newer vs older burs) has an effect on the fatigue failure load, number of cycles for failure, and survival rates of lithium disilicate glass-ceramic simplified restorations adhesively cemented to epoxy resin substrate reinforced by glass fiber. The tested hypothesis is that the increased bur experience (as a result of the milling sequence) would not affect the fatigue behavior of the ceramic restorations.

2. Materials and methods

2.1. Specimen assembly description

A simplified tri-layer setup was designed to simulate an occlusal restoration for a posterior tooth based on previous studies. The lithium disilicate disc reproducing the occlusal restoration was adhesively cemented onto a glass fiber reinforced epoxy resin disc as a dentin analogue (Chen et al., 2014; Kelly et al., 2010; Prochnow et al., 2018a,b; Venturini et al., 2018; Scherer et al., 2018; Monteiro et al., 2018).

2.2. Ceramic disc specimen preparation

Disc-shaped ceramic specimens with a diameter of 10 mm and 1.5 mm thickness were milled in the CAD/CAM system (CEREC inLab MC XL, Sirona, Bensheim, Germany) according to the methodology described by Fraga et al. (2015) using lithium disilicate blocks (Ivoclar Vivadent, Schaan, Liechtenstein). Three sets of burs (Step Bur and Cylinder Pointed Bur - 12 S, Cerec inLab, Sirona Dental Systems) were used to mill 18 ceramic discs each (simplified restorations; one set of burs milled 18 discs). The specimens were divided into 3 groups (n = 18) according to the increased bur experience (as a result of the milling sequence): **G1-6** – discs obtained from the 1st to 6th milling of each bur set; **G7-12** – specimens from the 7th to 12th milling; **G13–18** – discs from the 13th to 18th (Table 1).

After milling, the ceramic surface representing the occlusal side was polished with 180, 600 and 1200 grit silicon carbide (Norton Saint Gobain, São Paulo, Brazil) under water irrigation in a polishing machine (EcoMet 250 Grinder Polisher, Buehler, Lake Buff, IL, USA). After polishing, the discs were cleaned in an ultrasonic bath in isopropyl alcohol for 5 min and dried; lastly, they were crystalized as

Table 1
Study design.

Group's codes/Milling sequence	Testing Assembly	Burs Set 1	Burs Set 2	Burs Set 3	Sample Size (n)
G1-6	Discs of lithium-disilicate based ceramic (IPS e.max CAD, Ivoclar Vivadent) submitted to CAD/	1st to 6th milling			18
G7-12	CAM milling and adhesively cemented to dentin analogue substrate (fiber reinforced polymer,	7th to 12th milling			18
G13-18	Protec, São Paulo, Brazil)	13th to 18th milling			18

recommended by the manufacturer.

2.3. Surface roughness analysis

The surface roughness values were determined using a contact profilometer (MarSurf XT 20, Mahr-Goettingen, Germany) for all groups. Three measurements were performed for each specimen on the cementation surface. The Ra and Rz values were calculated from the average results of the three readings. The measures were performed with 0.8 mm cut-off and a transverse length of 0.25 mm.

2.4. Preparation of the epoxy resin discs

The discs made of glass fiber reinforced epoxy resin (Protec, São Paulo, Brazil) were obtained by slicing a rod into 2.0 mm-thick x 10 mm-diameter discs in a cutting machine (Isomet 1000, Buehler). Then the cylinders were cleaned with an ultrasonic bath in isopropyl alcohol for 5 min, dried, and randomly allocated into pairs with the ceramic discs.

2.5. Cementation procedures

The cementation surface of all the ceramic discs were etched with 5% hydrofluoric acid (HF) (Condac Porcelana 5%, FGM, Joinville, Brazil) for 20 s, as recommended by the manufacturer. After etching, they were rinsed for 30 s in water and gently air-dried. Then, the 10-Methacryloyloxydecyl dihydrogen phosphate (10_MDP) silane Monobond N (Ivoclar Vivadent) was applied on the surface using a microbrush (KG Sorensen, Cotia, São Paulo), allowing it to act for 60 s.

The cementation surface of the epoxy resin was etched with 10% HF (Condac Porcelana 10%, FGM) for 30 s, and then rinsed for 30 more seconds. One drop of each self-etching primer A and B of the resin cement system (Multilink N, Ivoclar Vivadent) were mixed and actively scrubbed with a microbrush on the dentin analogue surface for 20 s, and gently air-dried for 5 s.

After surface treatments, the resin cement (Multinlink N) pastes were mixed as recommended by the manufacturer and applied on the center of the treated ceramic surface and on its counterpart epoxy disc, followed by joining both and applying 7.5 N on the occlusal ceramic side using an adapted apparatus device. Then, the cement excesses were removed, and light-activation (1200 mW/cm^2, Bluephase N, Ivoclar Vivadent) was performed for five exposures of 20 s each (0°, 90°, 180°, 270°, and top from the occlusal side/ceramic). The samples were stored in distilled water in the incubator (Olidef, Ribeirão Preto, Brazil) at 37 °C for 7–14 days before the step-stress tests.

2.6. Stepwise fatigue tests

The specimens were subjected to an accelerated life test (stepwise method) (Instron ElectroPuls E3000, Instron Corporation, Norwood, MA, United States) (Anami et al., 2016; Carvalho et al., 2014; Magne et al., 2010; Zucuni et al., 2019; Venturini et al., 2019). The load was applied with a 40 mm diameter stainless-steel sphere in the center of the 'occlusal' ceramic surface supported by a flat steel base under water (Fig. 1). This test set-up was performed in order to obtain a failure pattern similar to that found clinically as observed in previous studies (Kelly et al., 2010; Monteiro et al., 2018), since it generates subsurface radial cracks (Kelly, 1999). Before testing, an adhesive tape (110 μm) was glued and a thin sheet of non-rigid material (cellophane, 2.5 μm) was placed on the occlusal side of all specimen surfaces to promote better stress distribution (Monteiro et al., 2018).

The stepwise loading design (Anami et al., 2016; Carvalho et al., 2014; Fennis et al., 2004; Güth et al., 2016) corresponds to a simulation of a clinical situation through cycling the samples with increasing load increments until material failure or up to a predetermined number of cycles. In this study, the specimens were tested with a 20 Hz frequency

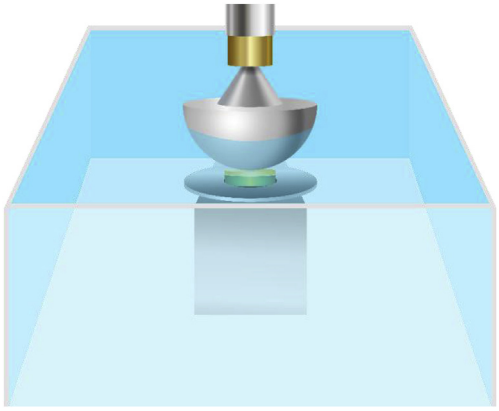

Fig. 1. Illustrative image of fatigue test set-up, where a stainless-steel sphere (40 mm in diameter) was used to apply the load at the center of the samples, submerged into water.

at an initial maximum load of 400 N for 5000 cycles to accommodate the testing assembly; after that, a step-size of 200 N and a lifetime of 20,000 cycles at each load step were used, with a maximum load ranging from 1000 N up to 2600 N until the survival or failure of the specimen in a distinct step. After each step-load, the samples were analyzed by light oblique transillumination to identify the presence of radial cracks, which was considered as failure. Then, fatigue failure load (FFL) and number of cycles for failure (CFF) data were recorded for statistical purposes.

2.7. Fractography analysis

After fracture, the specimens were cut perpendicularly to the crack line using a diamond saw at low speed (Isomet 1000, Buehler). Then, the cross-sectional surface was observed under stereomicroscope (Stemi 508, Carl Zeiss, Gena, Germany).

2.8. Residual stress analysis (DRX)

A residual stress analysis of the crystalline phase was performed using the milled surface of crystalized block leftovers of groups G1-6 and G12-18 prior to and after hydrofluoric acid conditioning using an X-ray diffractometer (Empyrean/Panalytical, The Netherlands) with a Cr tube (λ = 2.288796 Å). Scans were performed at 2Θ from 26°, 43°, 60° and 77°. The O peak displacement was analyzed with 113°, 114,5° and 115°, which corresponds to the planes (421), (153) and (440) of the lithium disilicate phase, with 10 s per scan step time and generator settings of 40 m Å and 40 kV (Ramos et al., 2016). As residual stress concentration causes a change in the crystal planes as a function of depth, and those changes will generate a shift in the obtained X-ray peaks during the different incident angles used in the analysis, one can infer the residual stress concentration present on a surface by checking X-ray peak shifts.

2.9. Statistical analysis

SPSS version 21 (SPSS Inc., Chicago, US) statistical software was used for all analyses. First, a descriptive analysis of surface roughness (Ra and Rz parameters), FFL and CFF was performed for obtaining mean and standard deviation values. After assuring a parametric and homoscedastic data distribution (Shapiro-Wilk and Levene tests) of all variables, the data were subjected to one-way ANOVA and post-hoc Tukey's test (α = 0.05). FFL and CFF data were additionally submitted to survival analysis (Kaplan-Meier and Mantel-Cox (log rank) tests) and the survival probabilities in each testing step were then tabulated.

Table 2
Results from surface roughness analysis (μm – Ra and Rz parameters, mean and standard deviation - SD), and fatigue tests (mean and 95% confidence intervals – CI for fatigue failure load – FFL and number of cycles for failure – CFF).

Group Codes	Surface Roughness		Fatigue test	
	Ra Mean (SD)	Rz Mean (SD)	FFL Mean (95% CI)	CFF Mean (95% CI)
G1-6	1.23 (0.07)[b]	6.55 (0.43)[b]	2,055 (1,900–2,210)[a]	130,555 (115,093–146,018)[a]
G7-12	1.46 (0.11)[a]	7.55 (0.62)[a]	1,944 (1,840–2,048)[a]	119,444 (109,026–129,861)[a]
G13–18	1.46 (0.14)[a]	7.55 (0.76)[a]	1,911 (1,832–1,990)[a]	116,111 (108,205–124,016)[a]

*Different letters in each column indicate statistical differences depicted by one-way ANOVA and Turkey's post-hoc tests.

Table 3
Survival rates for fatigue failure load and number of cycles for failure with respective standard errors.

Group Codes	Fatigue failure load (N)/Cycles for failure									
	400/5,000	1000/25,000	1200/45,000	1400/65,000	1600/85,000	1800/105,000	2000/125,000	2200/145,000	2400/165,000	2600/185,000
G1-6	1	1	1	1	0.78 (0.10)	0.61 (0.12)	0.56 (0.12)	0.28 (0.11)	0.06 (0.05)	0.0
G7-12	1	1	1	0.94 (0.05)	0.83 (0.08)	0.78 (0.10)	0.11 (0.07)	0.06 (0.05)	0.0	–
G13–18	1	1	1	1	0.89 (0.07)	0.56 (0.12)	0.11 (0.07)	0.0	–	–

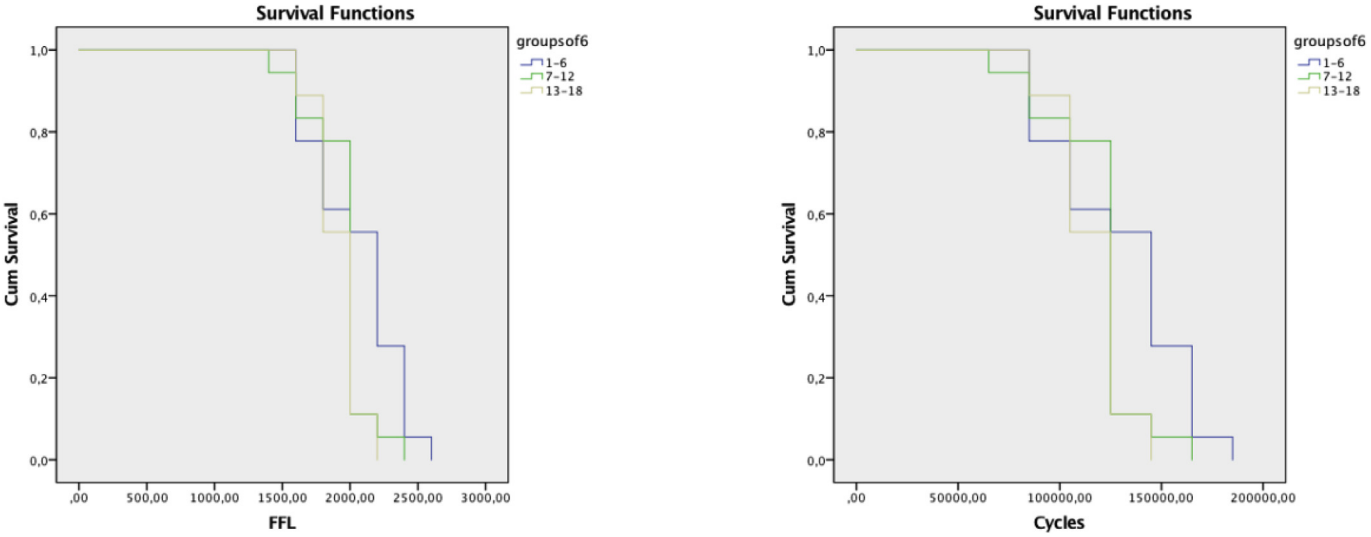

Fig. 2. Survival graphs for fatigue failure load (FFL) and number of cycles for failure (CFF) data obtained by survival analysis (Kaplan-Meier and Mantel-Cox log-rank tests).

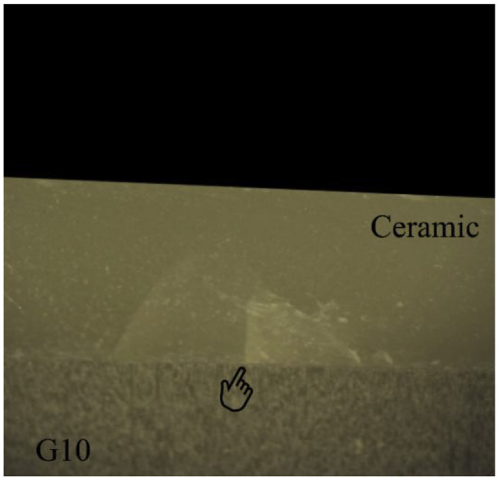

Fig. 3. Stereomicroscope image, showing the crack origin at the cementation interface.

3. Results

Surface roughness (Ra: $p < 0.001$; Rz: $p < 0.001$) was affected by milling sequence, as smoother surfaces were observed on the first six milled discs. Next, the roughness became similar and the milling sequence did not lead to alterations in this outcome (G7-12 and G13-18 presented similar Ra and Rz roughness values) (Table 2).

FFL and CFF were not influenced ($p = 0.21$) by milling sequence (Table 2). In terms of survival probabilities, it is observed that the groups behaved similarly, even though there was a distinct behavior at 2000 N/125,000 cycles: the G1-6 samples presented 56% survival probability, while the G7-12 and G13-18 samples had a rate of 11% (Table 3, Fig. 2).

Fractography analysis showed that all radial cracks initiated at the cementation surface without reaching the load application surface (Fig. 3).

The residual stress measured in the crystalline phase just after milling of the specimens was negligible based on the fact that no change in X-ray peak positions were observed (Fig. 4).

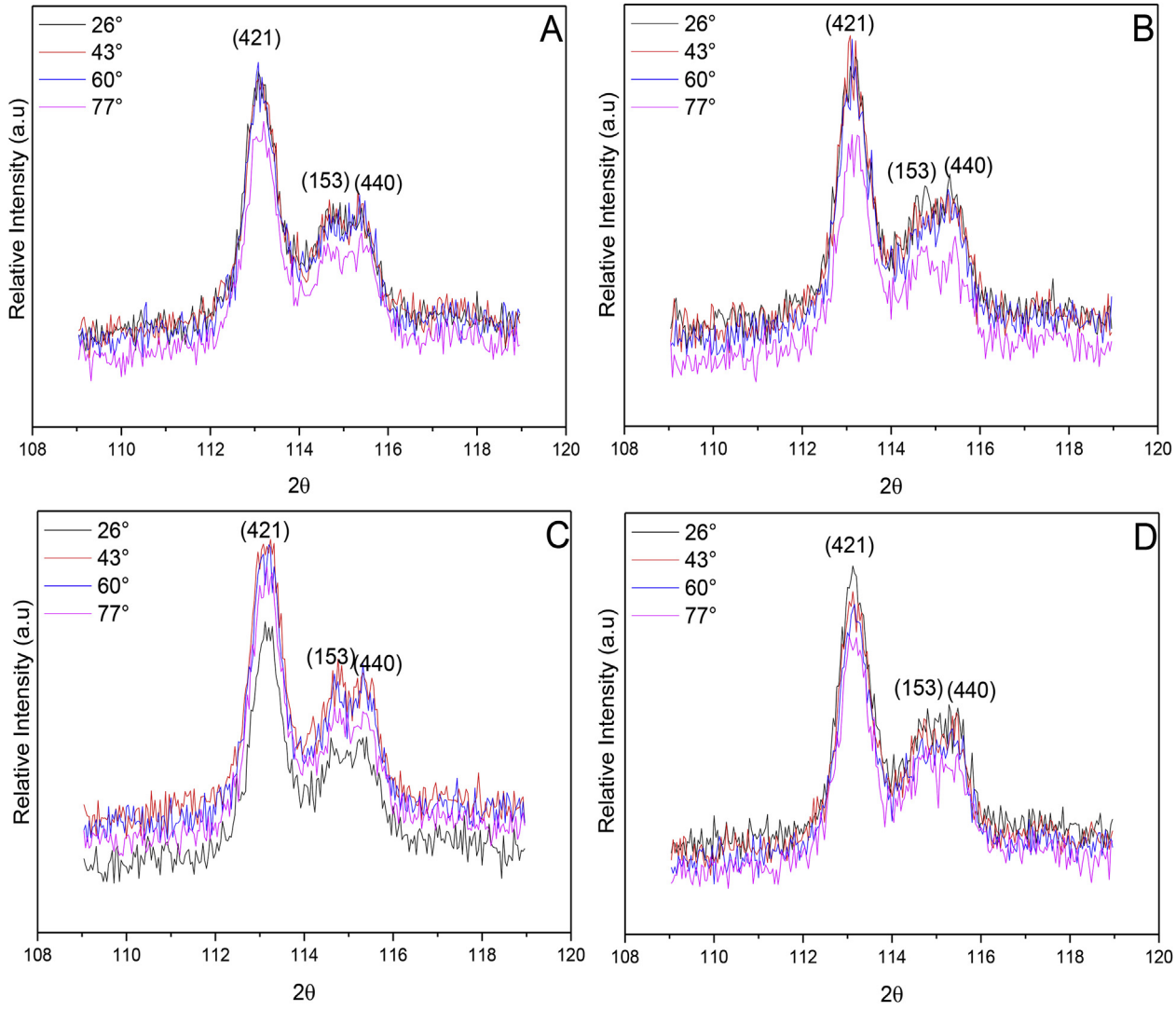

Fig. 4. X-ray diffractograms of non-etched milled (A and B) and etched specimens (C and D) at different incident angles, in which the peak positions remained the same.

4. Discussion

Based on the data obtained in the present study, it is clear that the increase in CAD/CAM bur experience (as a result of the milling sequence) did not affect either the fatigue failure load (FFL) or the number of cycles for failure (CFF) of lithium-disilicate based ceramics adhesively cemented to a dentin analogue substrate. Thus, the study hypothesis was confirmed. In addition, the residual stress concentration induced by milling was negligible. Despite this, a smoother surface (lower roughness) was depicted for the first six milled ceramic discs.

CAD/CAM milling of dental ceramics is mostly performed by removing materials with chipping/microchipping mechanisms (Sreejith and Ngoi, 2001). In summary, this process occurs by first inducing elastic deformation when the grinding instrument (diamond bur) contacts the ceramic (Fig. 5-A), as the load contact among these substrates increases plastic deformation initiates and residual stress accumulation increases (Fig. 5-B). Cracks are also introduced during plastic deformation, usually in a perpendicular relation to the cut region (Fig. 5-C). As the damage accumulates, a sub-critical crack growth mechanism occurs (Fig. 5-D). The next step is based on the initial occurrence of horizontal cracks (parallel to the cut region) and concentration of tensile stresses at subsurface and around cracks (Fig. 5-E). Finally, chipping of ceramic occurs (Fig. 5-F), although subsurface damage remains present (Marshall et al., 1983; Sreejith and Ngoi, 2001). It is noteworthy that crack formation is usually induced by an imbalance in the elastic-plastic deformation mechanism associated to the residual stress concentration (Marshall et al., 1983).

Most part of the energy involved for material removal during milling (1 - by the attrition between cutting instrument and ceramic; and 2 - by the surface/sub-surface deformation and crack induction) is released as thermal energy, i.e. increasing local temperature (Rekow and Thompson, 2005). This scenario results in high temperatures at the cutting region because ceramics present low thermal conductivity. Meanwhile, the concomitant cooling during milling to reduce and control the temperature may contribute to residual stress accumulation and subsurface damage (Rekow and Thompson, 2005). Therefore, the literature has already shown that milling triggers a cascade of events on the ceramic surface and subsurface resulting in radial and lateral cracks, chipping, damage, and residual stress introduction (Marshall et al., 1983; Rekow and Thompson, 2005; Sindel et al., 1998; Zhang et al., 1999). All of these factors lead to potential sites for fracture initiation and consequent failure of the respective restoration in a clinical environment (Rekow and Thompson, 2005; Sindel et al., 1998). However, our data supported that the increased bur experience (as a result of milling sequence) and the consequent triggered degradation from the grinding tool did not influence the aforementioned mechanism, and

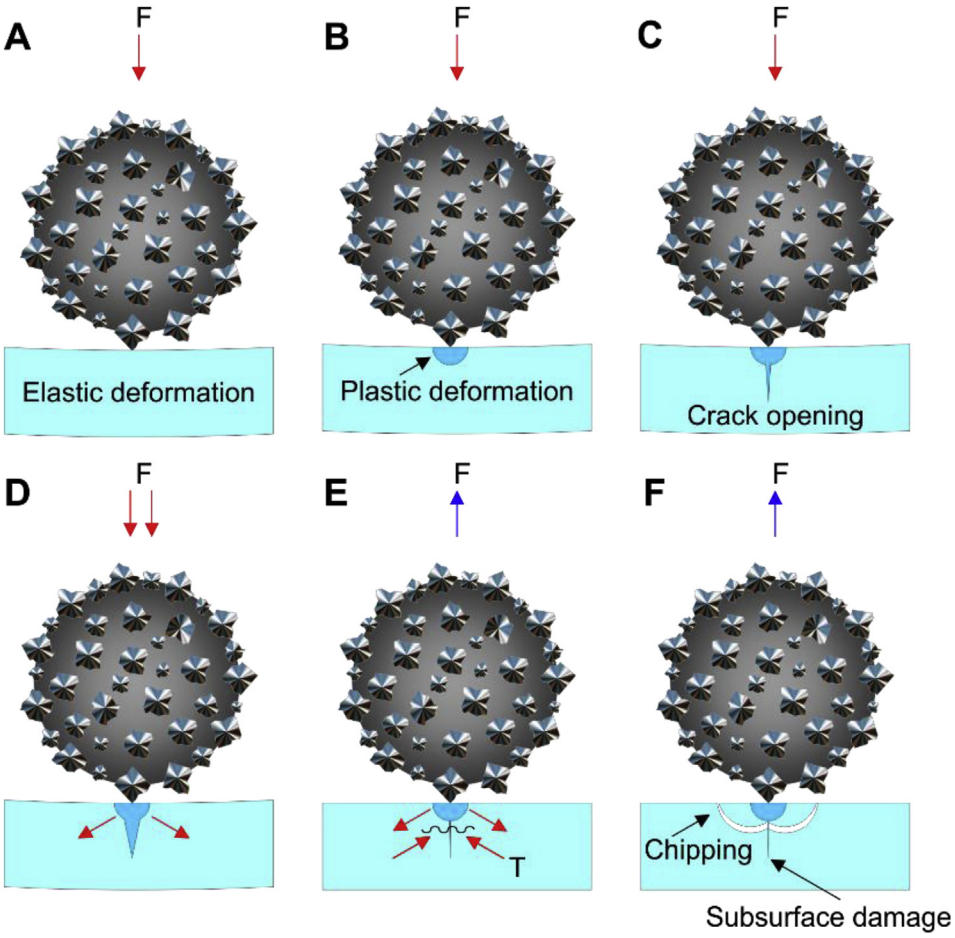

Fig. 5. Schematic figure describing the mechanism of cutting of ceramics with diamond burs during milling: A) Initial contact between cutting instrument and ceramic surface inducting elastic deformation; B) Increase of residual stress leading to plastic deformation; C) Vertical crack induction in response to residual stress concentration; D) Subcritical-crack growth of a vertical crack; E) Tensile residual stress appears in response to the occurrence of horizontal fissures; F) Chipping of the external surface material without exposing subsurface damage.

thus no effect on the fatigue behavior of the bonded ceramic restorations could be detected, as already found by previous studies (Madruga et al., 2019; Corazza et al., 2015).

The XRD analysis in the present study corroborates the aforementioned finding, since no residual stress could be found in the lithium disilicate crystal phase of conditioned and non-conditioned specimens. In the case of non-conditioned specimens, this was probably due to milling in the blue stage when the material is softer (Denry and Holloway, 2010), associated with the crystallization firing which releases residual stresses (Denry, 2013). Another possible explanation is the existence of microcracks on the subsurface (Rekow and Thompson, 2005), also leading to relaxation of residual stresses of the milled surface (Serbena and Zanotto, 2012).

Another important factor is that surface treatments are performed on the milled surface for bond improvements after milling. Murillo-Gómez et al. (2018) elucidated that etching with 5% hydrofluoric acid for 20 s (protocol used herein) acts until a depth of 57.4 ± 15.3 μm, promoting dissolution of glassy matrix. This influence could be enough to reduce any damage induced by milling, masking the effect of such a factor on the final surface, and consequently in the properties of adhesively bonded restorations. The amount of glass dissolution and the effect of acid etching will obviously depend on the ceramic microstructure considered, and the parameters used for the surface treatment such as hydrofluoric acid concentration and etching time (Murillo-Gómez et al., 2018; Addison et al., 2007).

Since ceramics are brittle materials, their mechanical properties are highly influenced by the surface flaw population (Kelly et al., 2010), especially when tensile stress concentration takes place. The masticatory intermittent loading from the oral environment results in tensile stress concentration at the intaglio surface (ceramic-cement-substrate interface), the exact region where most clinical failures occur (Anusavice and Hojjatie, 1992; Kelly, 1999; Kelly et al., 1990; Thompson et al., 1994; Zhang et al., 2013). Despite this, it is important to emphasize that fatigue and subcritical crack growth mechanisms are dependent on the time, load, and frequency, among others test parameters.

Regarding roughness, Addison et al. (2012) observed that milling sequence influenced the surface roughness, which is in accordance with the observations of the current study. Indeed, the final roughness of a milled material is inherently linked to the milling instrument cutting ability, and the cutting ability can be influenced by the lifespan of the instrument. Therefore, the lifespan of the burs may be decreased when milling harder materials (i.e. lithium disilicate ceramics) (Curran et al., 2017). Fraga et al. (2017) observed that the increase in roughness led to a deleterious impact on biaxial flexural strength under fatigue of lithium-disilicate ceramics, which was not corroborated by our data. The reason for such disagreement could be that this previous study did not consider the adhesive cementation effect. After cementation, surface defects are filled by the resin cement (de Kok et al., 2017), which enhances stress distribution and prevents crack openings from the ceramic intaglio surface, constituting a mechanism known as crack bridging (Wang et al., 2007; de Kok et al., 2017; Monteiro et al., 2018; Xiaoping et al., 2014).

Taking into consideration the inherent limitations of *in vitro* scenarios in mimicking the complexity of forces exerted during the masticatory function and the particularities of the intraoral environment, caution should be taken for clinical extrapolations from the findings of the current study.

5. Conclusions

- Fatigue behavior of adhesively cemented lithium-disilicate glass-ceramic restorations was not influenced by CAD/CAM bur experience (newer vs older in consequence of milling sequence).
- The residual stress concentration induced by milling was negligible.

Acknowledgements

This study did not receive any specific grant from funding agencies in the public, commercial, or not-for-profit sectors.

References

Addison, O., Cao, X., Sunnar, P., Fleming, G.J.P., 2012. Machining variability impacts on the strength of a “chair-side” CAD-CAM ceramic. Dent. Mater. 28 (8), 880–887. https://doi.org/10.1016/j.dental.2012.04.017.

Addison, O., Marquis, P.M., Fleming, G.J., 2007. The impact of hydrofluoric acid surface treatments on the performance of a porcelain laminate restorative material. Dent. Mater. 23, 461–468.

Alao, A.-R., Stoll, R., Song, X.-F., Miyazaki, T., Hotta, Y., Shibata, Y., et al., 2017 Jan. Surface quality of yttria-stabilized tetragonal zirconia polycrystal in CAD/CAM milling, sintering, polishing and sandblasting processes. J. Mech. Behav. Biomed. Mater. Netherlands 65, 102–116. https://doi.org/10.1016/j.jmbbm.2016.08.021.

Anami, L., Lima, J., Valandro, L., Kleverlaan, C., Feilzer, A., Bottino, M., 2016 Jan. Fatigue resistance of Y-TZP/Porcelain crowns is not influenced by the conditioning of the intaglio surface. Operat. Dent. 41 (1), E1–E12. https://doi.org/10.2341/14-166-L.

Anusavice, K., Hojjatie, B., 1992. Tensile stress in glass-ceramic crowns: effect of flaws and cement voids. Int. J. Prosthodont. (IJP) 5 (4), 345–350.

Beuer, F., Schweiger, J., Edelhoff, D., 2008 May. Digital dentistry: an overview of recent developments for CAD/CAM generated restorations. Br. Dent. J. 204 (9), 505–511. https://doi.org/10.1038/sj.bdj.2008.350.

Campos, F., Valandro, L., Feitosa, S., Kleverlaan, C., Feilzer, A., de Jager, N., et al., 2017. Adhesive Cementation Promotes Higher Fatigue Resistance to Zirconia Crowns. Operative Dentistryhttps://doi.org/10.2341/16-002-L.

Carvalho, A.O., Bruzi, G., Giannini, M., Magne, P., 2014 Apr. Fatigue resistance of CAD/CAM complete crowns with a simplified cementation process. J. Prosthet. Dent 111 (4), 310–317. https://doi.org/10.1016/j.prosdent.2013.09.020.

Chen, C., Trindade, F.Z., De Jager, N., Kleverlaan, C.J., Feilzer, A.J., 2014. The fracture resistance of a CAD/CAM Resin Nano Ceramic (RNC) and a CAD ceramic at different thicknesses. Dent. Mater. 30 (9), 954–962. https://doi.org/10.1016/j.dental.2014.05.018.

Corazza, P.H., de Castro, H.L., Feitosa, S.A., Kimpara, E.T., Della Bona, A., 2015. Influence of CAD-CAM diamond bur deterioration on surface roughness and maximum failure load of Y-TZP-based restorations. Am. J. Dent. 28 (2), 95–99.

Curran, P., Cattani-Lorente, M., Anselm Wiskott, H.W., Durual, S., Scherrer, S.S., 2017 Mar. Grinding damage assessment for CAD-CAM restorative materials. Dent. Mater. England 33 (3), 294–308. https://doi.org/10.1016/j.dental.2016.12.004.

de Kok, P., Pereira, G.K.R., Fraga, S., de Jager, N., Venturini, A.B., Kleverlaan, C.J., 2017. The effect of internal roughness and bonding on the fracture resistance and structural reliability of lithium disilicate ceramic. Dent. Mater. 33 (12), 1416–1425. https://doi.org/10.1016/j.dental.2017.09.018.

Denry, I., Holloway, J.A., 2010 Jan. Ceramics for Dental Applications: A Review. Materials (Basel), vol 3. Multidisciplinary Digital Publishing Institute (MDPI), pp. 351–368. https://doi.org/10.3390/ma3010351. 1.

Denry, I., Kelly, J.R., 2014 Dec. Emerging ceramic-based materials for dentistry. J. Dent. Res. United States 93 (12), 1235–1242. https://doi.org/10.1177/0022034514553627.

Denry, I., 2013. How and when does fabrication damage adversely affect the clinical performance of ceramic restorations? Dent. Mater. 29 (1), 85–96. https://doi.org/10.1016/j.dental.2012.07.001.

Fennis, W.M.M., Kuijs, R.H., Kreulen, C.M., Verdonschot, N., Creugers, N.H.J., 2004. Fatigue resistance of teeth restored with cuspal-coverage composite restorations. Int. J. Prosthodont. (IJP) 17 (3), 313–317.

Fraga, S., Amaral, M., Bottino, M.A., Valandro, L.F., Kleverlaan, C.J., May, L.G., 2017. Impact of machining on the flexural fatigue strength of glass and polycrystalline CAD/CAM ceramics. Dent. Mater. 33 (11), 1286–1297. https://doi.org/10.1016/j.dental.2017.07.019.

Fraga, S., Valandro, L.F., Bottino, M.A., May, L.G., 2015. Hard machining, glaze firing and hydrofluoric acid etching: do these procedures affect the flexural strength of a leucite glass-ceramic? Dent. Mater. 31 (7), e131–e140. https://doi.org/10.1016/j.dental.2015.04.005.

Güth, J.-F., Edelhoff, D., Goldberg, J., Magne, P., 2016 Jan. CAD/CAM polymer vs direct composite resin core buildups for endodontically treated molars without ferrule. Operat. Dent. 41 (1), 53–63. https://doi.org/10.2341/14-256-L.

Jokstad, A., 2017 Apr. Computer-assisted technologies used in oral rehabilitation and the clinical documentation of alleged advantages - a systematic review. J. Oral. Rehabil. England 44 (4), 261–290. https://doi.org/10.1111/joor.12483.

Kelly, J.R., Giordano, R., Pober, R., Cima, M.J., 1990. Fracture surface analysis of dental ceramics: clinically failed restorations. Int. J. Prosthodont. (IJP) 3 (5), 430–440.

Kelly, J.R., Nishimura, I., Campbell, S.D., 1996 Jan. Ceramics in dentistry: historical roots and current perspectives. J. Prosthet. Dent. United States; 75 (1), 18–32.

Kelly, J.R., Rungruanganunt, P., Hunter, B., Vailati, F., 2010. Development of a clinically validated bulk failure test for ceramic crowns. J. Prosthet. Dent 104 (4), 228–238. https://doi.org/10.1016/S0022-3913(10)60129-1.

Kelly, J.R., 1999. Clinically relevant approach to failure testing of all-ceramic restorations. J. Prosthet. Dent 81 (6), 652–661. https://doi.org/10.1016/S0022-3913(99)70103-4.

Lebon, N., Tapie, L., Vennat, E., Mawussi, B., 2015 Aug. Influence of CAD/CAM tool and material on tool wear and roughness of dental prostheses after milling. J. Prosthet. Dent. United States 114 (2), 236–247. https://doi.org/10.1016/j.prosdent.2014.12.021.

Li, R.W.K., Chow, T.W., Matinlinna, J.P., 2014 Oct. Ceramic dental biomaterials and CAD/CAM technology: state of the art. J. Prosthodont. Res. Netherlands 58 (4), 208–216. https://doi.org/10.1016/j.jpor.2014.07.003.

Madruga, C.F.L., Bueno, M.G., Dal Piva, AM. de O., Prochnow, C., Pereira, G.K.R., Bottino, M.A., et al., 2019 Mar. Sequential usage of diamond bur for CAD/CAM milling: effect on the roughness, topography and fatigue strength of lithium disilicate glass ceramic. J. Mech. Behav. Biomed. Mater. 91, 326–334. https://doi.org/10.1016/j.jmbbm.2018.12.037.

Magne, P., Schlichting, L.H., Maia, H.P., Baratieri, L.N., 2010 Sep. In vitro fatigue resistance of CAD/CAM composite resin and ceramic posterior occlusal veneers. J. Prosthet. Dent 104 (3), 149–157. https://doi.org/10.1016/S0022-3913(10)60111-4.

Marshall, D.B., Evans, A.G., Yakub, B.T.K., Tien, J.W., Kino, G.S., 1983. The nature of machining damage in brittle materials. Proc. Roy. Soc. Lond.: Math. Phys. Eng. Sci. 385 (1789), 461475. https://doi.org/10.1098/rspa.1983.0023.

Monteiro, J.B., Oliani, M.G., Guilardi, L.F., Prochnow, C., Rocha Pereira, G.K., Bottino, M.A., et al., 2018. Fatigue failure load of zirconia-reinforced lithium silicate glass ceramic cemented to a dentin analogue: effect of etching time and hydrofluoric acid concentration. J. Mech. Behav. Biomed. Mater. 77, 375–382. https://doi.org/10.1016/J.JMBBM.2017.09.028.

Murillo-Gómez, F., Palma-Dibb, R.G., De Goes, M.F., 2018. Effect of acid etching on tridimensional microstructure of etchable CAD/CAM materials. Dent. Mater. 34 (6), 944–955. https://doi.org/10.1016/j.dental.2018.03.013.

Prochnow, C., Pereira, G.K.R., Venturini, A.B., Scherer, M.M., Rippe, M.P., Bottino, M.C., Kleverlaan, C.J., Valandro, L.F., 2018a. How does hydrofluoric acid etching affect the cyclic load-to-failure of lithium disilicate restorations? J. Mech. Behav. Biomed. Mater. 87, 306–311.

Prochnow, C., Venturini, A.B., Guilardi, L.F., Pereira, G.K.R., Burgo, T.A.L., Bottino, M.C., et al., 2018b. Hydrofluoric acid concentrations: effect on the cyclic load-to-failure of machined lithium disilicate restorations. Dent. Mater. https://doi.org/10.1016/j.dental.2018.06.028.

Ramos, N. de C., Campos, T.M.B., Paz IS, de La, Machado, J.P.B., Bottino, M.A., Cesar, P.F., et al., 2016 Jul. Microstructure characterization and SCG of newly engineered dental ceramics. Dent. Mater. 32 (7), 870–878. https://doi.org/10.1016/j.dental.2016.03.018.

Rekow, D., Thompson, V.P., 2005 Jul. Near-surface damage–a persistent problem in crowns obtained by computer-aided design and manufacturing. Proc Inst Mech Eng H. England 219 (4), 233–243. https://doi.org/10.1243/095441105X9363.

Scherer, M.M., Prochnow, C., Venturini, A.B., Pereira, G.K.R., Burgo, T.A.L., Rippe, M.P., 2018. Valandro LF Fatigue failure load of an adhesively-cemented lithium disilicate glass-ceramic: conventional ceramic etching vs etch & prime one-step primer. Dent. Mater. 34 (8), 1134–1143.

Serbena, F.C., Zanotto, E.D., 2012. Internal residual stresses in glass-ceramics: a review. J. Non-Cryst. Solids. https://doi.org/10.1016/j.jnoncrysol.2012.01.040.

Sindel, J., Petschelt, A., Grellner, F., Dierken, C., Greil, P., 1998 May. Evaluation of subsurface damage in CAD/CAM machined dental ceramics. J. Mater. Sci. Mater. Med. 9 (5), 291–295.

Sreejith, P.S., Ngoi, B.K.A., 2001. Material removal mechanisms in precision machining of new materials. Int. J. Mach. Tool Manuf. 41 (12), 1831–1843. https://doi.org/10.1016/S0890-6955(01)00014-1.

Suresh, S., 1991. Fatigue of Materials, Cambridge Solid State Science Series. Press Syndicate of the University of Cambridge, Cambridge.

Teixeira, E.C., Piascik, J.R., Stoner, B.R., Thompson, J.Y., 2007 Jun. Dynamic fatigue and strength characterization of three ceramic materials. J. Mater. Sci. Mater. Med. 18 (6), 1219–1224. https://doi.org/10.1007/s10856-007-0131-4.

Thompson, J.Y., Anusavice, K.J., Naman, a, Morris, H.F., 1994. Fracture surface characterization of clinically failed all-ceramic crowns. J. Dent. Res. 73 (12), 1824–1832. https://doi.org/10.1177/00220345940730120601.

Venturini, A.B., Prochnow, C., May, L.G., Kleverlaan, C.J., Valandro, L.F., 2017. Fatigue failure load of feldspathic ceramic crowns after hydrofluoric acid etching at different concentrations. J. Prosthet. Dent. https://doi.org/10.1016/j.prosdent.2017.03.021.

Venturini, A.B., Prochnow, C., Pereira, G.K.R., Segala, R.D., Kleverlaan, C.J., Valandro, L.F., 2019 Jan 25. Fatigue performance of adhesively cemented glass-, hybrid- and resin-ceramic materials for CAD/CAM monolithic restorations. Dent. Mater. https://doi.org/10.1016/j.dental.2019.01.013. ([In-press, corrected proof]).

Venturini, A.B., Prochnow, C., Pereira, G.K.R., Werner, A., Kleverlaan, C.J., Valandro, L.F., 2018. The effect of hydrofluoric acid concentration on the fatigue failure load of adhesively cemented feldspathic ceramic discs. Dent. Mater. 34 (4), 667–675.

Wang, Y., Katsube, N., Seghi, R.R., Rokhlin, S.I., 2007. Statistical failure analysis of adhesive resin cement bonded dental ceramics. Eng. Fract. Mech. 74 (12), 1838–1856. https://doi.org/10.1016/j.engfracmech.2006.11.006.

Wendler, M., Belli, R., Valladares, D., Petschelt, A., Lohbauer, U., 2018. Chairside CAD/CAM materials: part 3: cyclic fatigue parameters and lifetime predictions. Dent. Mater. 34 (6), 910–921.

Xiaoping, L., Dongfeng, R., Silikas, N., 2014. Effect of etching time and resin bond on the

flexural strength of IPS e.max Press glass ceramic. Dent. Mater. 30 (12). https://doi.org/10.1016/j.dental.2014.08.373. e330–6.
Zhang, Q.H., Zhang, J.H., Jia, Z.X., Sun, J.L., 1999. Material-removal-rate analysis in the ultrasonic machining of engineering ceramics. J. Mater. Process. Technol. 88 (1). https://doi.org/10.1016/S0924-0136(98)00400-2.
Zhang, Y., Lawn, B.R., Malament, K.A., Van Thompson, P., Rekow, E.D., 2006. Damage accumulation and fatigue life of particle-abraded ceramics. Int. J. Prosthodont. United States 19 (5), 442–448.
Zhang, Y., Sailer, I., Lawn, B.R., 2013. Fatigue of dental ceramics. J. Dent. 41 (12), 1135–1147. https://doi.org/10.1016/j.jdent.2013.10.007.
Zucuni, C.P., Venturini, A.B., Prochnow, C., Rocha Pereira, G.K., Valandro, L.F., 2019 Feb. Load-bearing capacity under fatigue and survival rates of adhesively cemented yttrium-stabilized zirconia polycrystal monolithic simplified restorations. J. Mech. Behav. Biomed. Mater. 90, 673–680.